PRECAMBRIAN PIKE'S PEAK IRON-FORMATION, CENTRAL ARIZONA

by
Roger M. Slatt, Greta M. Heintz,
Patrick H. Lowry, and Patrick F. O'Hara

Department of Geology
Arizona State University
Tempe, Arizona

INTRODUCTION

The Pike's Peak iron-formation is the largest of a discontinuous series of iron deposits, about 120 km long by 60 km wide, within the Precambrian Yavapai Series of central Arizona (fig. 1). The Pike's Peak deposit consists of a series of lenticular bodies of interlaminated chert and iron oxide which form an outcrop belt about 6 km long by 700 m wide within more areally extensive phyllites and associated meta-volcanic rocks.

Precambrian iron-formations occur worldwide (James and Sims, 1973). Although it is generally agreed that they are the products of chemical sedimentation, the many published accounts have emphasized their regional extent, economic potential, and petrology rather than their sedimentology and stratigraphy. The Pike's Peak iron-formation is no exception. Farnham and Havens (1957) and Harrer (1964) provided generalized information on the economic potential and geology of the deposit. Sharp (1963) investigated its magnetic properties.

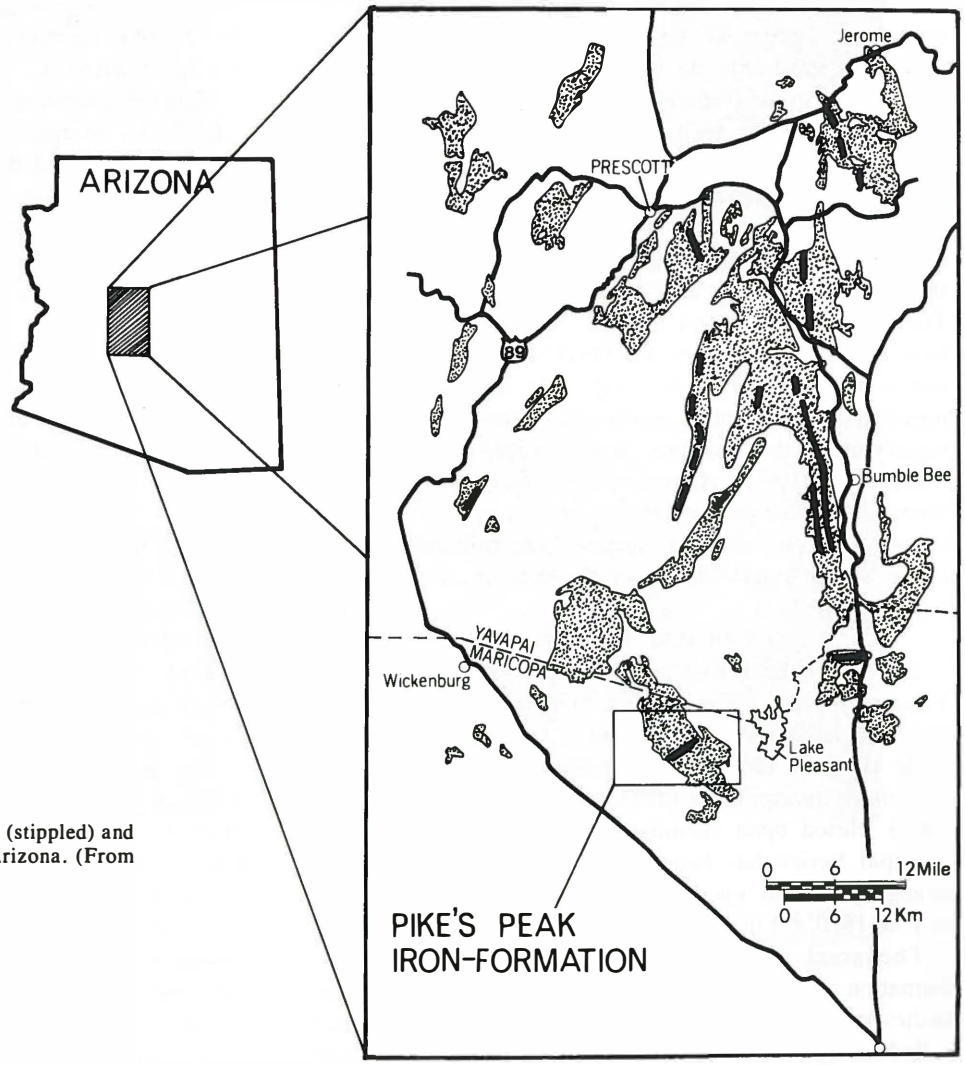

Figure 1. Distribution of Yavapai Series (stippled) and iron-formation (solid lines) in central Arizona. (From Harrer, 1964.)

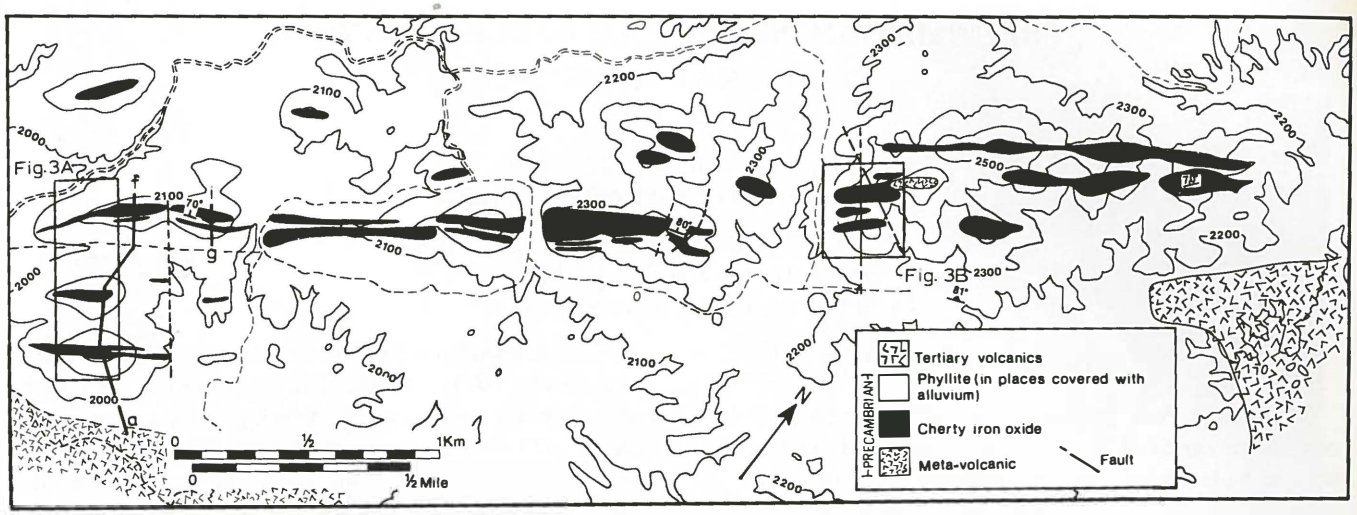

Figure 2. Geologic map of the Pike's Peak iron-formation and associated lithologies. Contour intervals are in feet.

Bayley and James (1973) included a brief description in their review of iron-formations of the United States.

The intent of this field guide and the field trip is to summarize current knowledge of the Pike's Peak iron-formation, especially its sedimentology and stratigraphy. The field trip will leave Tempe and proceed north on highway I-17, then west on the Carefree Highway (74), to about 7 miles west of the Lake Pleasant turnoff. Here, an unmarked dirt road leads to the iron-formation.

The field trip will consist of examining outcrops of the iron-formation and associated lithologies in the two areas shown in figures 3A and 3B (see fig. 2 for locations). These areas are reached by dirt roads (fig. 2). The features to be examined are described below. This information is preliminary in nature and is the result of mapping, measuring stratigraphic sections, and cursorily examining about 35 thin sections, supplemented by X-ray diffraction analysis. A general summary of the iron-formation is also presented along with a hypothesis of the depositional environment. Detailed interpretation of the origin and geologic history of the deposit awaits further work.

GENERAL GEOLOGY

The Pike's Peak iron-formation comprises part of the Yavapai Series, a complex of metamorphosed volcanic and associated rocks more than 6 km thick, which include rhyolite, diorite, greenstone, phyllite, schist, amphibolite, quartzite, argillite, and graywacke (Harrer, 1964). Based upon radiometric age determinations, the Yavapai Series has been formally defined as a time-stratigraphic unit encompassing the period 1770 ± 10 m.y. to 1820 ± 1 m.y. (Anderson and others, 1971).

The areal distribution of the Pike's Peak iron-formation is shown in figure 2. It occurs as lenticular bodies of laminated chert and iron oxide beds, hereafter called cherty iron oxide, which range in width from 15 to 100 m, which are rarely continuous for more than 350 m along strike, and which form resistant ridges more than 200 m higher than adjacent valleys (figs. 3A and B). Beds strike approximately N.60°E. and dip steeply toward the northwest.

Phyllite underlies valleys between cherty iron oxide ridges, and occupies lower ridge slopes (figs. 3A and B); occasionally phyllite forms a small hill. The phyllite generally is silver-gray in color with a prominent, steeply-dipping, axial plane cleavage (fig. 3F). A whitish-gray phyllite containing coarser clasts, hereafter called sandy phyllite, occurs locally. Phyllites weather to a variety of colors.

Along mid- and upper-slopes of ridges, the cherty iron oxide and phyllite are interbedded (figs. 3D and E). Here, the cherty iron-oxide occurs as small lenses, giving rise to a pinch-and-swell character (fig. 3E). Some lenses are folded (fig. 4F).

Other lithologies are not common in the area. Thin beds of gray calcite, interlaminated with chert and iron oxide (fig. 4C), occur locally. Meta-volcanic rocks are found south of the iron-formation and are interbedded with cherty iron oxide along one ridge-top (fig. 2). Gray bedded chert occurs near the meta-volcanics in one area. Dikes of Tertiary andesite porphyry (?) and coarse quartz veins cross-cut the iron-formation at several locales.

The iron-formation is dissected by many small faults which trend obliquely to the regional strike and which often form small saddles or terraces within resistant ridges. The faults are recognizable by small breccia zones (fig. 4E), occasional slickensides, and displacement of individual beds. Offset appears to be minor. Owing to the difficulty in recognizing small fault breccias and minor offsets, more faults probably occur than are shown in figure 2.

No evidence was found to suggest the cherty iron

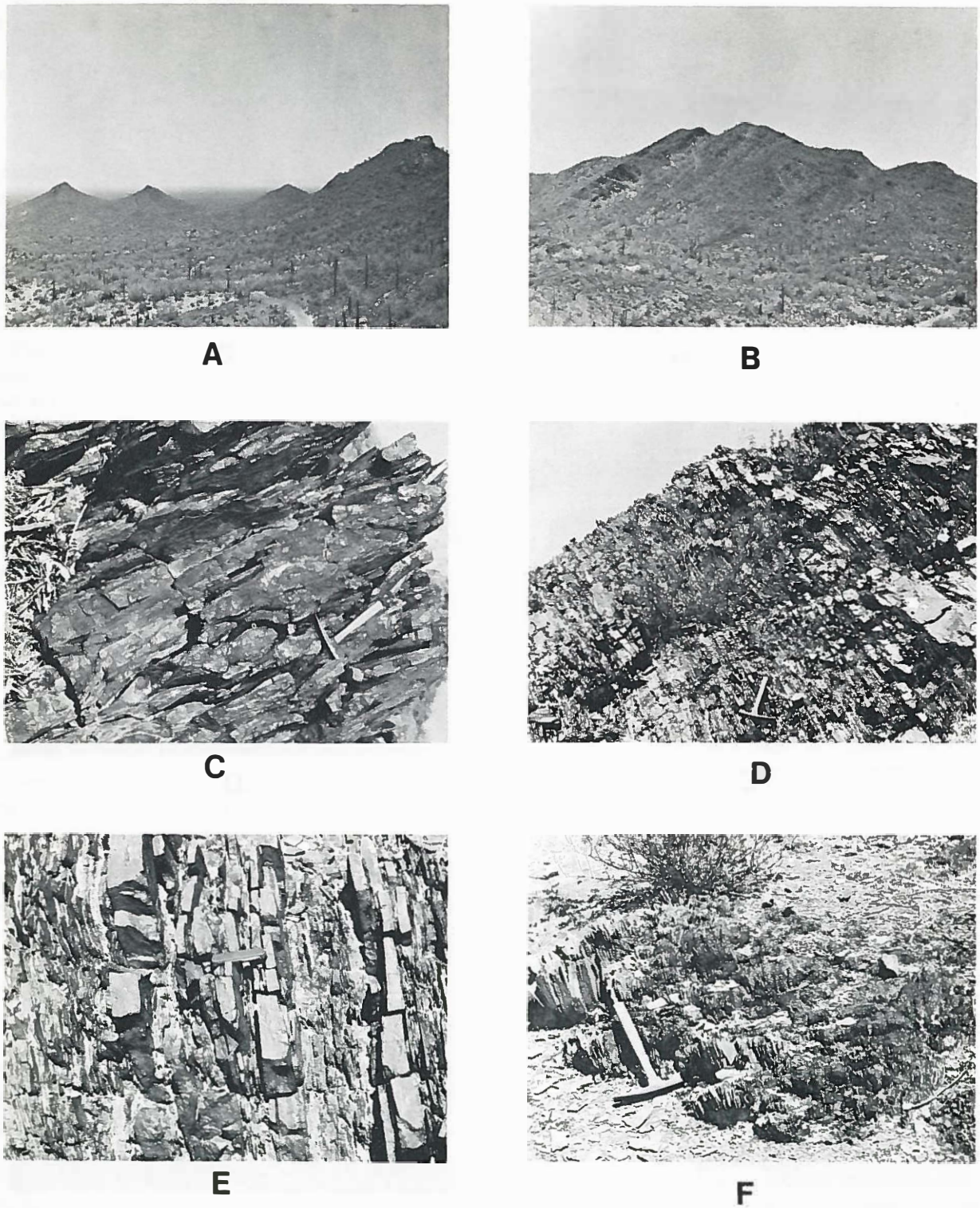

Figure 3. (A) View looking southwest at ridges of iron-formation. See fig. 2 for location. (B) View looking northeast at ridges of iron-formation. See fig. 2 for location. (C) Side, or internal view of bed of massive cherty iron oxide. Note pod structure below hammer. Top of the ridge is toward the upper right. (E) Close-up view of interbedded cherty iron oxide (resistant lenticular beds) and phyllite. Knife is about 8 cm in length. Top of the photo is toward the right. (F) View of phyllite outcrop showing axial plane cleavage.

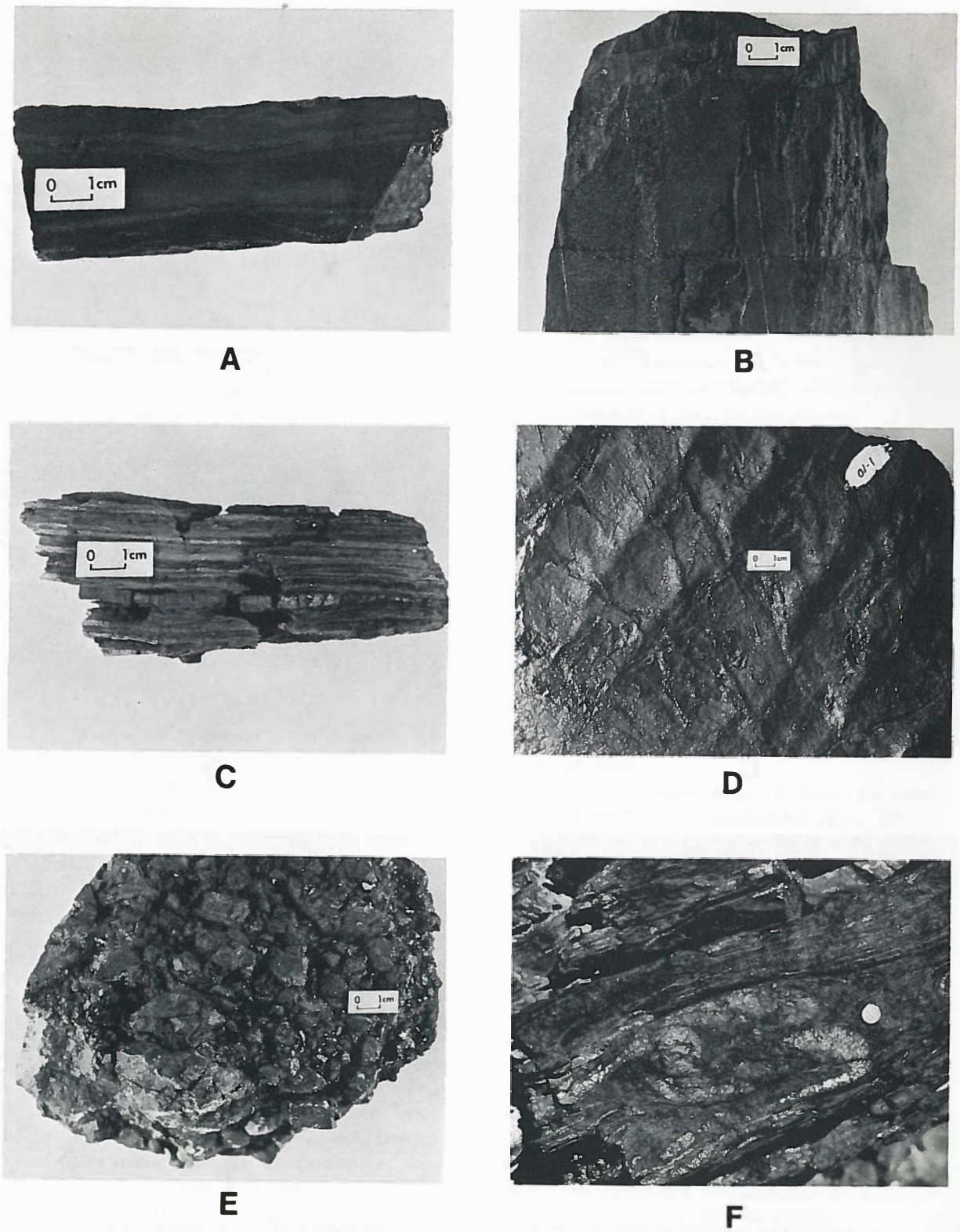

Figure 4. (A) Polished slab showing two thin hematite laminae between chert laminae. (B) Slaty cherty iron oxide with two linear grooves oriented about 350°. (C) Laminated carbonate lithology containing a small lense of hematite. (D) Ripple-like features on a bedding plane. (E) Fault breccia. (F) Side, or internal view of folded cherty iron oxide.

oxide ridges are repeated by folding within the outcrop area of the iron-formation, even though beds of cherty iron oxide are sometimes folded (fig. 4F).

STRATIGRAPHY

Because of a lack of evidence for repetition of beds by folding or faulting, the ridges of cherty iron oxide and intervening valleys underlain by phyllite are assumed to form a continuous stratigraphic sequence. Two stratigraphic sections were measured. (See fig. 2 for locations.) Section a-f (fig. 5) extends from the meta-volcanics northwestward across three cherty iron oxide ridges (fig. 3A). The measured thickness of 930 m represents a maximum thickness due to some folding of beds (figs. 3C and 4F). Section g-i (fig. 6) crosses one major cherty iron oxide ridge. The measured thickness of 270 m also represents a maximum possible value. The total thickness of the iron-formation and associated lithologies was not measured, so it presently is unknown.

At Section a-f, cherty iron oxide occurs in three separate horizons within thicker sections of phyllite (fig. 5). The highest horizon at Section a-f is correlative with the one cherty iron oxide horizon measured at Section g-i (fig. 6). Silver-gray phyllite is most common throughout the sections; sandy phyllite is restricted to the lower third of Section a-f.

Zones of interbedded cherty iron oxide and phyllite are most frequent near beds of massive cherty iron oxide (without interbedded phyllite). Visual estimates of the proportions of the two lithologies, taken at intervals ranging from 3 to 10 m along Section g-i (fig. 6), indicate there is a systematic increase in the proportion of cherty iron oxide interbeds, at the expense of phyllite, as beds of massive cherty iron oxide are approached. Although similar measurements were not made at Section a-f, the same systematic variation was noted.

The three horizons of iron-formation (fig. 5) appear to record three major cycles of sedimentation.

PETROLOGY

CHERTY IRON OXIDE

In outcrop, most of the cherty iron oxide has a blocky or massive appearance. It consists of planar to lenticular laminae of alternating quartz (occasionally jasper) and hematite which range from less than 1 to greater than 35 mm in thickness (fig. 4A); quartz laminae normally are thickest.

In thin section, the cherty laminae comprise a mosaic of polygonal, equidimensional to elongate, interlocking quartz crystals which range in size from about 0.03 to 0.20 mm (fig. 7A). Thin bands of differing crystal size often are adjacent to one another. Fine hematite crystals

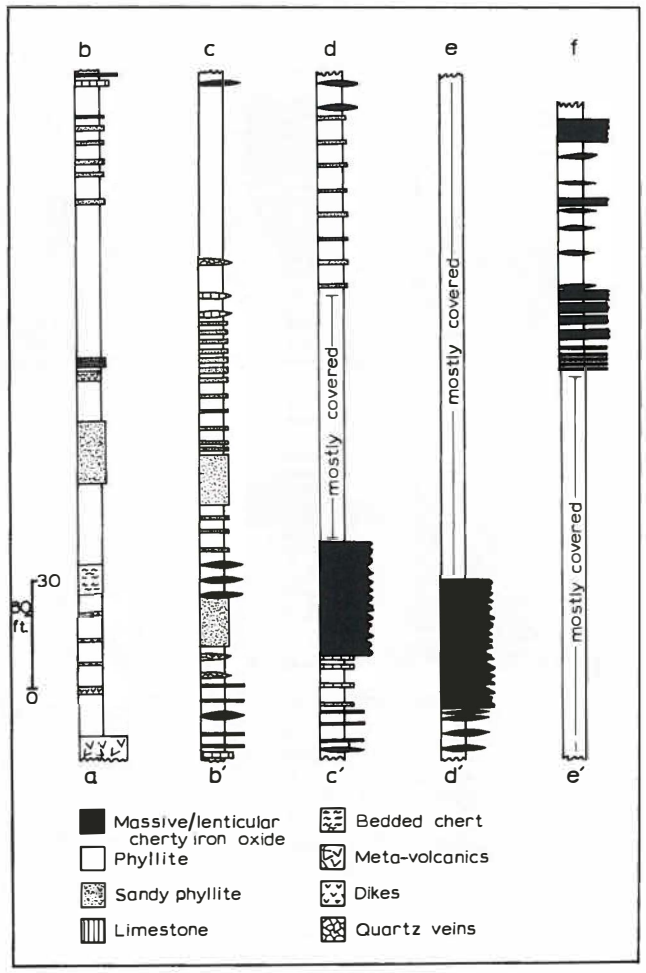

Figure 5. Measured stratigraphic section a–f. See fig. 2 for location.

are aligned within chert laminae; red jasper laminae contain the greatest proportion of hematite. Feldspar, calcite, muscovite, and biotite are also minor constituents; the latter two normally are oriented parallel to laminae.

Boundaries between chert and hematite laminae are sharp (fig. 7B). The hematite laminae are composed principally of fine granular hematite, in places weathering to limonite and goethite, with minor dispersed quartz, muscovite, and biotite. Magnetite, reported by Harrer (1964), generally is not present in sufficient quantities to be detected by X-ray diffraction analysis.

Some of the cherty iron oxide has a slaty (rather than blocky or massive) appearance (fig. 4B). In thin section, the slaty-oxide lithology tends to be more micaceous, to exhibit good schistosity, and to contain larger quartz crystals (> 0.30 mm); small quantities of magnetite are detectable by X-ray diffraction.

PHYLLITE

The phyllite is composed of chlorite, calcite, muscovite, albite, quartz, opaques, and stilpnomelane (?) (fig. 7D).

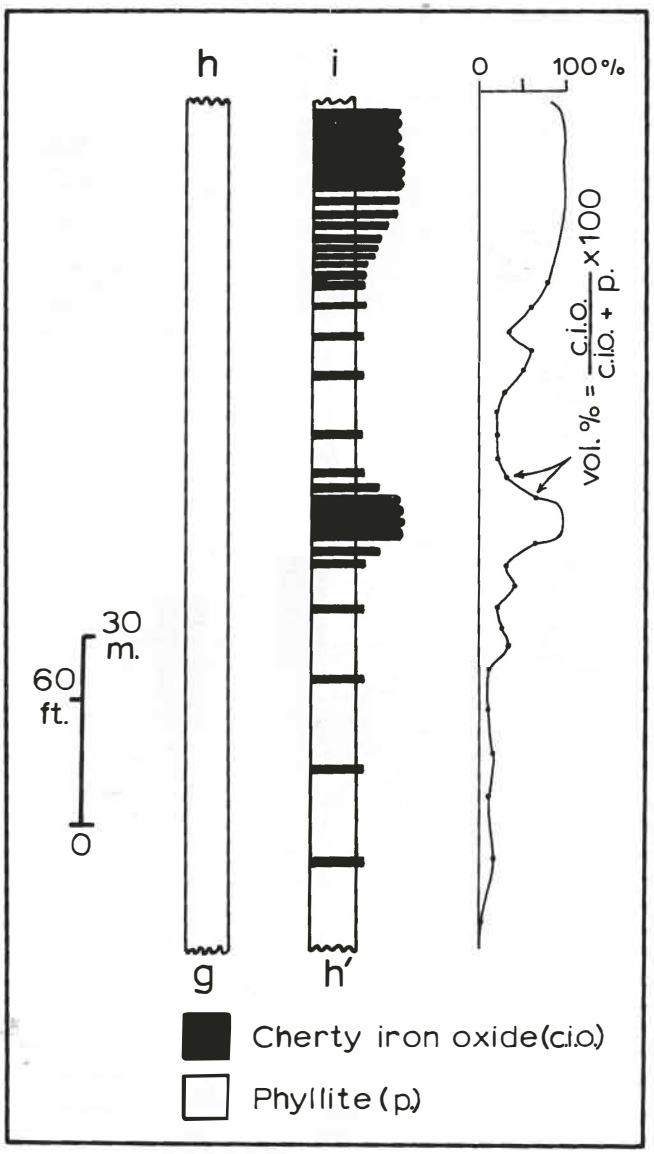

Figure 6. Measured stratigraphic section g–i. See fig. 2 for location. Volume % = proportion of cherty iron oxide in cherty iron oxide/phyllite interbeds. Data points mark intervals and stratigraphic locations of visual estimates.

The micaceous minerals define a schistose foliation. The sandy phyllite is similar, but it also contains scattered, larger grains of quartz (fig. 7E) which are clearly visible in hand specimen.

CARBONATE

The carbonate rock is composed of thin laminae of gray calcite, rust-gray chert, and steel gray-black, lenticular hematite (fig. 4C). In thin section, the calcite is finely-crystalline (fig. 7C) and contains elongate aggregates of hematite which either are oriented parallel to laminations or define micro-folds. Quartz grains and muscovite needles are minor constituents. Both chert and hematite laminae are similar to those of cherty iron oxide.

META-VOLCANICS

The meta-volcanic rocks are dark green with flattened, white streaks parallel to foliation. They are of intermediate (?) composition, having been altered to an assemblage of chlorite, muscovite, calcite, quartz, and opaques (fig. 7F). Some relict clinopyroxene (?), hornblende (?), and plagioclase can be seen in thin section.

CHEMISTRY

Partial chemical analyses of cherty iron oxide samples (Farnham and Havens, 1957) are compared in table 1 with average chemical compositions of other iron-formations (James, 1966). The Pike's Peak deposit is relatively enriched in Mn and Al_2O_3, particularly when compared with other hematite-rich iron-formations. The high Mn content is present in pyrolusite, which occurs in sufficient quantities to be detected by X-ray diffraction analysis. The Al_2O_3 content probably reflects the occurrence of micas.

Harrer (1964) reports the presence of 0.01–0.1 percent Co, Ni, Ti, and Cu and 0.001–0.01 percent V in a cherty iron oxide sample.

TABLE 1. COMPARATIVE CHEMISTRY OF PIKE'S PEAK AND OTHER IRON-FORMATIONS.

	A	B	C	D	E	F	G	H
SiO_4	43.9	33.1	44.8	34.0	36.7	37.6	34.1	31.2
Al_2O_3	0.75	2.77	2.73	1.42	6.90	4.7	3.9	4.1
CaO	0.32	1.48	1.70	1.97	0.13	1.0	1.2	1.1
Fe	38.0	36.7	27.3	25.6	20.0	30.6	32.5	31.2
Mn	0.03	0.59	2.1	1.2	Tr	2.7	3.9	2.8
P	0.04	0.11	0.10	0.14	0.09	0.14	0.12	0.13
S	0.01	0.09	0.22	0.06	21.6	0.04	0.06	0.05

A. Hematite-rich iron formation (moderately metamorphosed). James (1966), Table 10, analyses A-K.
B. Magnetite-rich iron formation. James (1966), Table 12, analyses A-L.
C. Silicate-rich iron formation. James (1966), Table 14, analyses A-K.
D. Siderite-rich iron formation. James (1966), Table 17, analyses A-P.
E. Sulfide-rich iron formation, James (1966), Table 18, analysis A.
F. Surface trench samples, Pike's Peak iron formation. Farnham and Havens (1957), Table 2; several analyses.
G. Underground samples, Pike's Peak iron formation. Farnham and Havens (1957), Table 2; several analyses.
H. Overall composite of surface trench and underground samples, Pike's Peak iron formation. Farnham and Havens (1957), Table 2.

DEFORMATION AND METAMORPHISM

The Pike's Peak iron-formation has undergone at least one episode of deformation. The cherty iron oxide shows evidence of isoclinal folding (fig. 4F) while phyllites exhibit an axial plane cleavage (fig. 3F). Details of the deformation history await further investigation.

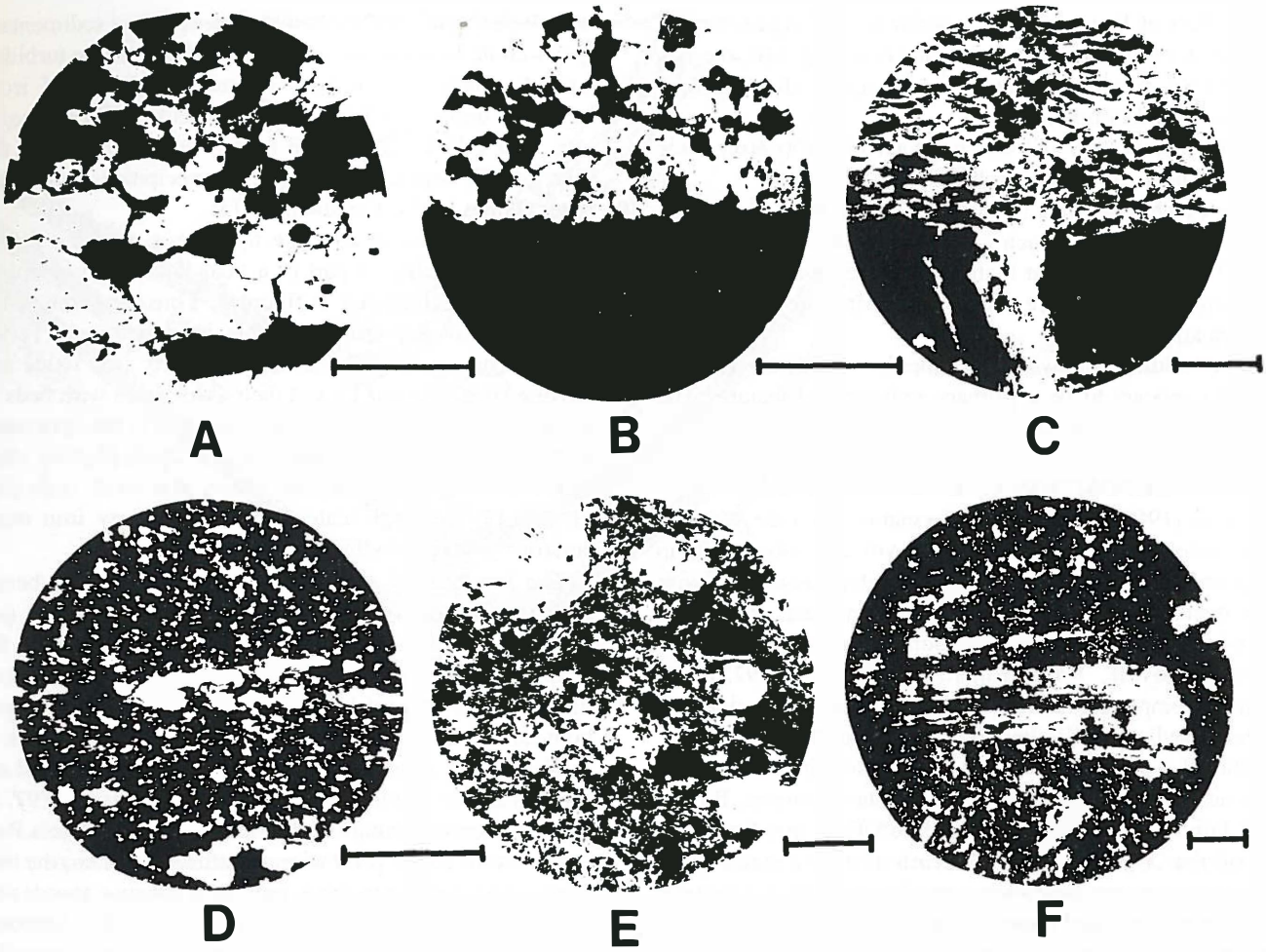

Figure 7. (A) Thin section of chert laminae showing variations in size of mosaic quartz crystals. Black mineral is hematite. Plane polarized and reflected light. (B) Thin section showing sharp contact between upper chert lamination and lower hematite lamination. Plane polarized and reflected light. (C) Thin section of upper calcite lamination and lower hematite lamination. Black elongate mineral in calcite is hematite. The vertical fracture in the hematite lamination is filled with calcite. Plane polarized and reflected light. (D) Thin section of phyllite. Note the band of quartz which appears to be folded. Plane polarized light. (E) Thin section of sandy phyllite. Plane polarized light. (F) Thin section of meta-volcanic. Note the altered plagioclase. Plane polarized light. Bar scale is 250 μm for A–F.

The mineral assemblage of the phyllite indicates the rocks have undergone regional prograde metamorphism to chlorite grade. The foliation defined by micaceous minerals (fig. 7D) is due to pre- or syn-tectonic recrystallization in the quartz-albite-muscovite-chlorite subfacies of the greenschist facies. The phyllites were probably shales, mudstones, and sandy mudstones prior to metamorphism.

The mosaic of polygonal quartz crystals which comprise chert laminae (fig. 7A) is typical of recrystallized quartz in cherty iron-formations (Mukhopadhyay and Chanda, 1972). Sizes of recrystallized quartz have been used by James (1955), Klein (1973), and others as an indicator of metamorphic grade in iron-formations. This was not possible for the Pike's Peak iron-formation because of the wide variety of crystal sizes present within single chert laminae (figs. 7A and B). Recrystallization of cherty iron oxide has obliterated any primary sedimentary textures that may have been present.

DEFORMATION AND SEDIMENTARY STRUCTURES

Gross (1972) described and illustrated a variety of primary sedimentary textures and structures common to iron-formations. These include granules and oolites, nodules, microbreccias, scour-and-fill structures, ripple marks, shrinkage cracks, and penecontemporaneous convolute folds. Listed below are similar structures found in the Pike's Peak deposit, but which we ascribe mainly to deformation.

(1) Sets of symmetrical ripples on bedding planes (fig. 4D); when viewed in cross-section, their internal structure is seen to be the result of compressional pinching of cherty iron oxide laminae.

(2) Folds which appear to be convoluted (fig. 4F); fold limbs usually are parallel, suggesting a deformation origin.

(3) What appear to be desiccation cracks in hematite laminae (fig. 7C) possibly are micro-fractures.

(4) Sets of linear grooves, similar to tool marks, on the undersides of slaty cherty iron oxide beds (fig. 4B); the sets are always parallel and perfectly straight, indicating they formed after lithification.

(5) Breccias (fig. 4E) which cut across cherty iron oxide beds, indicating they are fault breccias.

(6) Pinch-and-swell features of cherty iron oxide beds (figs. 3D and E), which resemble rippled beds; Beukes (1973) attributes similar features to diagenetic shrinkage of an original gel. More likely these are the product of deformation.

Interbedding of phyllite and cherty iron oxide (figs. 3D and E) appears to be a primary sedimentary feature. The origin of these interbeds is discussed below.

DEPOSITIONAL ENVIRONMENT

Gross (1965) classified iron-formations into the *Algoma*-type associated with volcanic and volcaniclastic rocks in eugeosynclinal belts, and the *Superior*-type associated with continental shelf sediments. Other proposed origins for iron-formation include deposition in lacustrine environments (Govett, 1966; Eugster and Chou, 1973) and penecontemporaneous replacement of shallow marine calcareous sediment (Kimberley, 1974; Dimroth, 1977b).

Based upon the stratigraphic association of iron-formation with meta-volcanics and meta-sediments, Bayley and James (1973) suggested the Pike's Peak iron-formation is of the *Algoma*-type. Dimroth (1977a) claims that *Algoma*-type iron-formations are characteristically lenticular bodies of parallel laminated beds that are associated with volcanic, turbidite and pelagic sediments. He suggests iron-formations are intercalated between turbidites, thus they were chemically precipitated on turbidite fans during periods of cessation of clastic sedimentation.

The Pike's Peak iron-formation exhibits these features, so a similar origin could be proposed. Phyllites and sandy phyllites may be metamorphosed distal and proximal turbidites. If so, then at least three major cycles of turbidite sedimentation are recorded in the measured stratigraphic Section a-f (fig. 6). Each cycle would terminate by the gradual transition from clastic to chemical sedimentation, as evidenced by the progressive development of cherty iron oxide beds at the expense of phyllite within cherty iron oxide horizons (fig. 7). The source of iron and silica could have been submarine volcanism (Goodwin, 1956 and 1973; Trendall and Blockley, 1970) or upwelling deep ocean water (Holland, 1973; Drever, 1974).

There are two obstacles to this origin. First, the typical radial growth pattern of submarine fans usually prevents superimposition of successively younger fans (Nelson and Nilson, 1974), thus contradicting the apparent cyclicity of the Pike's Peak deposit. However, not all turbidites are deposited on fans. For example, trench turbidites are transported axially, thus hindering development of prominent fans (Piper, et al., 1973). In addition, apparent sedimentary cycles could be preserved by a series of coalescing turbidite fans. Secondly, of the four sedimentary facies of iron-formation defined by James (1954)—oxide, carbonate, silicate, and sulfide—the oxide facies, which comprises the Pike's Peak deposit, is thought to precipitate in shallow water (James, 1954; Goodwin, 1973).

We propose, as an alternate hypothesis, that the Pike's Peak iron-formation is part of a tidal flat/deltaic complex. The model is illustrated in figure 8. Three features of the iron-formation are critical to this interpretation: (1) the common occurrence of interbeds of cherty iron oxide and phyllite (figs. 3D and E) and their association with beds of massive cherty iron oxide (figs. 5 and 6), (2) the systematic increase in proportion of cherty iron oxide to phyllite interbeds toward the more massive cherty iron oxide beds (fig. 6), and (3) the large-scale cyclicity of cherty iron oxide horizons between phyllite (fig. 6).

The interbeds of cherty iron oxide and phyllite bear a striking physical resemblance to tidal flat deposits (see Ginsburg, 1975 for several examples). A typical tidal flat sequence grades vertically from a shallow sub-tidal sand, into low-tide/inter-tidal sand and mud interbeds, then into high-tidal flat muds (Klein, 1975). Iron oxide oolites of shallow water origin are common in unmetamorphosed and low-grade iron-formations (Gross, 1972; Dimroth, 1977a), so it is conceivable that hematite laminae of the Pike's Peak deposit were oolitic prior to recrystallization. If so, the beds of massive cherty iron oxide may be analogous to sub-tidal oolite sand, while the cherty iron oxide/phyllite interbeds are analogous to inter-tidal deposits. Systematic variations in lithologies, as observed between cherty iron oxide and phyllite (fig. 6), also are characteristic of tidal flat sequences.

A tidal origin for the deposit requires both clastic and chemical sedimentation to occur in close proximity. Although the Precambrian depositional setting probably was not equivalent, bog iron deposits (James, 1966) may provide a partial modern analog. Slatt (1970) and Hoskin and Slatt (1972) describe an example of bog iron being precipitated on a clastic tidal flat. Also, it has been suggested that bacteria aided in the precipitation of iron-formation (Cloud, 1973), as is known to be the case in the production of bog iron (Harder, 1919; Pringsheim, 1949). Other examples of mixed clastic/chemical tidal flat deposits include limestone/sandstone (Shinn, 1973), dolomite/shale (Hoffman, 1975) and evaporite/mud (Thompson, 1975).

Our model accounts for the cyclicity of the Pike's Peak iron-formation by assuming tidal flat sedimentation occurred upon a delta surface. Deltaic sedimentation is often cyclic (Maill, 1976). One cycle consists of seaward progradation of a delta lobe followed by channel abandonment, subsidence, and marine transgression. Subsequently, a new delta lobe is deposited upon that of the earlier cycle. Each

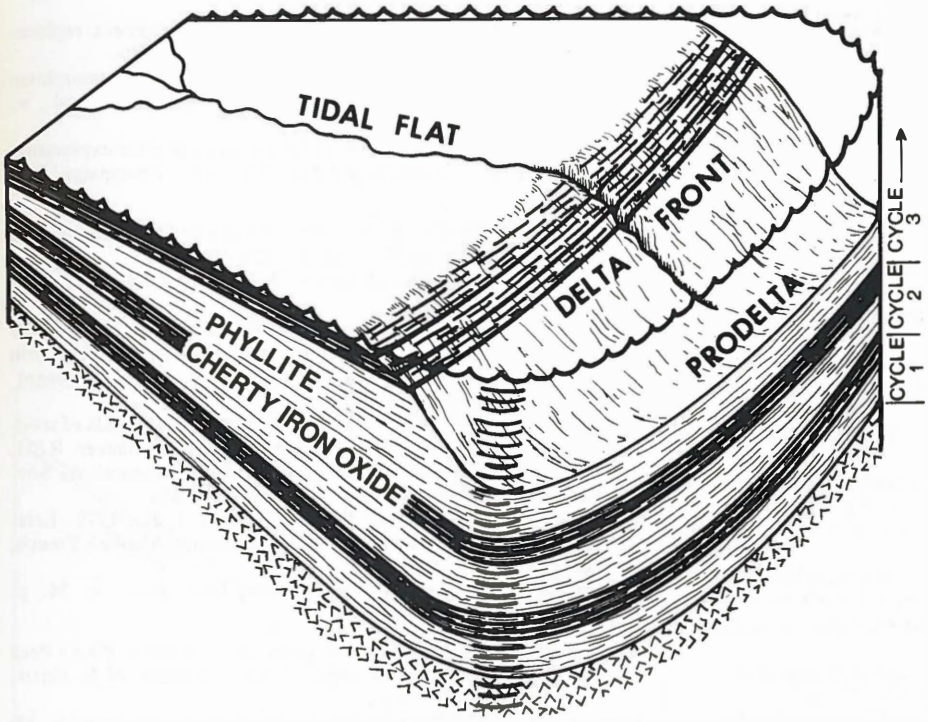

Figure 8. Model for the origin of the Pike's Peak iron-formation.

cycle may generate a stratigraphic sequence between 50 and 150 m or more in thickness, which is similar to the thickness between cherty iron oxide horizons of the Pike's Peak deposit (fig. 5).

In summary, we suggest that at least three cycles of deltaic sedimentation led to the development of the Pike's Peak deposit. Each cycle of sedimentation is represented by prodelta and delta front phyllites overlain by tidal flat cherty iron oxide. Chemical sedimentation in very shallow water might indicate the iron was derived from terrestrial chemical weathering (James, 1954; Lepp and Goldich, 1964).

ECONOMIC GEOLOGY

The Pike's Peak iron-formation is covered by 72 mining claims (Harrer, 1964). Preliminary assessment by Kaiser, Co., Inc. indicates iron resources of 100 million tons to an inferred depth of 130 m. If other occurrences of iron-formation are included (fig. 1), the low-grade iron resources within the mineralized belt of the Yavapai Series exceed this value (Harrer, 1964).

Average grade of ore is about 31 percent Fe (table 1). Because of low iron and high silica content, ore would have to be concentrated for commercial exploitation. Farnham and Havens (1957) describe several possible methods of increasing recovery and grade of the ore. The deposit could be mined by open pit methods.

ACKNOWLEDGMENTS

We express our appreciation to Kaiser Steel Corporation (Oakland, California office) for allowing us access to their property, to Michael Ward (Arizona State University) for first showing the Pike's Peak iron-formation to Slatt, and to Edmund Stump (Arizona State University) and William Jones (Kaiser Steel Corp.) for helpful suggestions and advice. Heintz and O'Hara were financially supported by Research Assistantships from Arizona State University's College of Liberal Arts.

REFERENCES CITED

Anderson, C. A., Blacet, P. M., Silver, L. T., and Stern, T. W., 1971, Revision of Precambrian stratigraphy in the Prescott-Jerome area, Yavapai County, Arizona, U.S. Geol. Surv. Bull. 1324-C, p. C1-C16.

Bayley, R. W. and James, H. L., 1973, Precambrian iron-formations of the United States, Econ. Geol. v. 68, p. 934–959.

Beukes, N. J., 1973, Precambrian iron-formations of southern Africa, Econ. Geol., v. 68, p. 960–1004.

Cloud, P., 1973, Paleoecological significances of the banded iron-formation, Econ. Geol., v. 68, p. 1135–1143.

Dimroth, E., 1977a, Facies models 5. Models of physical sedimentation of iron formations, Geosci. Canada, v. 4, p. 23–30.

——, 1977b, Facies models 6. Diagenetic facies of iron formation, Geosci. Canada, v. 4, p. 83–88.

Drever, J. I., 1974, Geochemical model for the origin of Precambrian banded iron formations, Bull. Geol. Soc. Amer., v. 85, p. 1099–1106.

Eugster, H. P., and Chou, I., 1973, The depositional environments of Precambrian banded iron-formations, Econ. Geol. v. 68, p. 1144–1168.

Farnham, L. L., and Havens, R., 1957, Pike's Peak iron deposits, Maricopa County, Arizona, U.S. Bur. Mines Rept. Inv. 5319, 31 p.

Ginsburg, R.N. (ed.), 1975, Tidal deposits, Springer-Verlag, N.Y., 428 p.

Goodwin, A.M., 1956, Facies relations in the Gunflint Iron Formation, Econ. Geol., v. 51, p. 565–595.

——, 1973, Archean iron-formations and tectonic basins of the Canadian Shield, Econ. Geol., v. 68, p. 915–933.

Govett, G. J. S., 1966, Origin of banded iron formations, Bull. Geol. Soc. Amer. v. 77, p. 1191–1212.

Gross, G. A., 1965, Geology of iron deposits in Canada, Vol. 1, General geology and evaluation of iron deposits, Canada Geol. Survey Econ. Geol. Rept. 22, 181 p.

——, 1972, Primary features in cherty iron-formations, Sediment. Geol., v. 7, p. 241–261.

Harder, E. C., 1919, Iron-depositing bacteria and their geological relations, U.S. Geol. Survey Prof. Paper 113, 89 p.

Harrer, C. M., 1964, Reconnaissance of iron resources in Arizona, U. S. Bur. Mines Inf. Circ. 8236, 204 p.

Hoffman, P., 1975, Shoaling-upward shale-to-dolomite cycles in the Rocknest Formation (Lower Proterozoic), Northwest Territories, Canada, *in* Ginsburg, R. N. (ed), Tidal Deposits, Springer-Verlag, N.Y., p. 257–265.

Holland, H. D., 1973, The oceans: a possible source of iron in iron-formations, Econ. Geol., v. 68, p. 1169–1172.

Hoskin, C. M. and Slatt, R. M., 1972, Iron in surface and subsurface waters, Grizzly Bar, southeastern Alaska, Univ. Alaska Inst. Water Resources Publ. No. IWR-29, 15 p.

James, H. L., 1954, Sedimentary facies of iron-formation, Econ. Geol., v. 49, p. 235–293.

——, 1955, Zones of regional metamorphism in the Precambrian of northern Michigan, Bull. Geol. Soc. Amer., v. 66, p. 1455–1488.

——, 1966, Chemistry of the iron-rich sedimentary rocks, U.S. Geol. Survey Prof. Paper 440-W, p. W1-W61.

James, H. L. and Sims, P. K., 1973, Precambrian iron-formations of the world, Econ. Geol., v. 68, p. 913–914.

Kimberley, M. M., 1974, Origin of iron ore by diagenetic replacement of calcareous oolite, Nature, v. 250, p. 319–320.

Klein, C., 1973, Changes in mineral assemblages with metamorphism of some banded Precambrian iron-formations, Econ. Geol., v. 68, p. 1075–1088.

Klein, G. de V., 1975, Sandstone depositional models for exploration for fossil fuels, Continuing Educ. Publ. Co., Champaign, Ill., 109 p.

Lepp, H., and Goldich, S. S., 1964, Origin of Precambrian iron formations, Econ. Geol., v. 58, p. 1025–1061.

Maill, A. D., 1976, Facies Models 4. Deltas, Geosci. Canada, v. 3, p. 215–227.

Mukhopadhyay, A. and Chanda, S. K., 1972, Silica diagenesis in the banded hematite jasper and bedded chert associated with the iron ore group of Jamda-Koira Valley, Orissa, India, Sediment. Geol., v. 8, p. 113–135.

Nelson, C. H. and Nilsen, T. H., 1974, Depositional trends of modern and ancient deep sea fans, *in* Dott, R. H. and Shaver, R. H. (eds.), Modern and ancient geosynclinal sedimentation, Soc. Econ. Paleon. Mineral. Spec. Publ. 19, p. 56–68.

Piper, D. J. W., von Huene, R., and Duncan, J. R., 1973, Late-Quaternary sedimentation in the active eastern Aleutian Trench, Geology, v. 1, p. 19–22.

Pringsheim, E. G., 1949, Iron bacteria, Biol. Rev., v. 24, p. 200–245.

Sharp, R. R., 1963, Some magnetic properties of a part of Pike's Peak iron deposit, Maricopa County, Arizona, unpubl. M.S. thesis, Univ. of Arizona, 115 p.

Shinn, E. A., 1973, Sedimentary accretion along the leeward, SE coast of Qatar Peninsula, Persian Gulf, *in* Purser, N.H. (ed), The Persian Gulf, Springer-Verlag, N.Y., 471 p.

Slatt, R. M., 1970, Sedimentological and geochemical aspects of sediment and water from ten Alaskan valley glaciers, unpubl. Ph.D. thesis, Univ. Alaska, 125 p.

Thompson, R. W., 1975, Tidal-flat sediments of the Colorado River Delta, northwestern Gulf of California, *in* Ginsburg, R. N., (ed) Tidal Deposits, Springer-Verlag, N.Y., p. 57–66.

Trendall, A. F. and Blockley, J. G., 1970, The iron formation of the Precambrian Hamersley Group, Western Australia, West. Australia Geol. Survey Bull. 119, 353 p.